Yoo et al. Molecular Medicine (2023) 29:156
https://doi.org/10.1186/s10020-023-00751-1

Molecular Medicine

RESEARCH ARTICLE

Open Access

Loss of Krüppel-like factor-10 facilitates the development of chemical-induced liver cancer in mice

Sung Hwan Yoo[1†], Ji Hae Nahm[2†], Woon Kyu Lee[3], Hyun Woong Lee[1], Hye Young Chang[4] and Jung Il Lee[1*]

Abstract

Background Krüppel-like factor 10 (KLF10) is involved in a positive feedback loop that regulates transforming growth factor β (TGFβ) signaling, and TGFβ plays an important role in the pathogenesis of liver disease. Here, we investigated whether *KLF10* deletion affects the development of liver fibrosis and hepatocellular carcinoma (HCC).

Methods We induced *KLF10* deletion in C57BL/6 mice. Liver fibrosis was induced by feeding a diet high in fat and sucrose (high-fat diet [HFD]), whereas HCC was produced by intraperitoneal administration of N-diethylnitrosamine (DEN). An in vitro experiment was performed to evaluate the role of KLF10 in the cancer microenvironment using Hep3B and LX2 cells. An immunohistochemical study of KLF10 expression was performed using human HCC samples from 60 patients who had undergone liver resection.

Results *KLF10* deletion resulted in an increased DEN-induced HCC burden with significant upregulation of *SMAD2*, although loss of KLF10 did not alter HFD-induced liver fibrosis. DEN-treated mice with *KLF10* deletion exhibited increased levels of mesenchymal markers (*N-cadherin* and *SNAI2*) and tumor metastasis markers (*matrix metalloproteinases 2* and *9*). *KLF10* depletion in Hep3B and LX2 cells using siRNA was associated with increased invasiveness. Compared with co-culture of *KLF10*-preserved Hep3B cells and *KLF10*-intact LX2 cells, co-culture of *KLF10*-preserved Hep3B cells and *KLF10*-depleted LX2 cells resulted in significantly enhanced invasion. Low KLF10 expression in resected human HCC specimens was associated with poor survival.

Conclusion The results of this study suggest that loss of KLF10 facilitates liver cancer development with alteration in TGFβ signaling.

Keywords Hepatocellular carcinoma, KLF10, Liver fibrosis, TGFβ

†Sung Hwan Yoo and Ji Hae Nahm have contributed equally to this work.

*Correspondence:
Jung Il Lee
mdflorence@yuhs.ac
[1] Department of Internal Medicine, Gangnam Severance Hospital, Yonsei University College of Medicine, 211 Eonju-Ro, Gangnam-Gu, Seoul 06273, Republic of Korea
[2] Department of Pathology, Gangnam Severance Hospital, Yonsei University College of Medicine, Seoul 06273, Republic of Korea
[3] Laboratory of Developmental Genetics, Department of Biomedical Sciences, Inha University College of Medicine, Incheon 22212, Republic of Korea
[4] Medical Research Center, Gangnam Severance Hospital, Seoul 06230, Republic of Korea

Introduction

Chronic liver injury caused by infectious, inflammatory, and metabolic disorders may result in liver fibrosis, the strongest risk factor for hepatocellular carcinoma (HCC) (Alter and Seeff 2000; Caldwell et al. 2004). Although nearly 90% of HCCs develop in cirrhotic livers (Llovet et al. 2021), fewer than 5% of patients with cirrhosis undergo progression to HCC annually (West et al. 2017). Despite recent advances in the understanding of the molecular pathogenesis of HCC and the identification of driver mutations, the key mechanisms involved in HCC development from cirrhosis are unclear.

Transforming growth factor β (TGFβ) plays an important role in the development of liver fibrosis and HCC by altering the composition of the microenvironment (Fabregat et al. 2016; Lee et al. 2016). TGFβ plays key roles in the plasticity of hepatic stellate cells and macrophages, which are the two major cells involved in liver fibrosis (Dewidar et al. 2019). TGFβ plays a dual role in HCC development; it suppresses tumor development in early stages and promotes tumor progression in later stages (Caja et al. 2007; Russell et al. 1988; Valdes et al. 2004; Wilkes et al. 2005). The mechanisms involved in shifting the role of TGFβ from tumor suppression to the regulation of tumor progression require further investigation.

The Krüppel-like factor (KLF) family shares a three-C_2H_2 zinc finger DNA-binding domain with a Krüppel linker between the zinc fingers (VHS Chang et al. 2012). One KLF family member, the human homologue of KLF10 (also known as the TGFβ-inducible early gene 1 [TIEG1]), is the product of a TGFβ-inducible early-response gene in osteoblastic cells (Subramaniam et al. 1995). KLF10 is involved in a positive feedback loop that regulates TGFβ signaling by inducing *SMAD2* expression and inhibiting the expression of the inhibitory *SMAD7* gene (Johnsen et al. 2002a; Johnsen et al. 2002b). Additionally, an increased intracellular level of KLF10 facilitates the anti-proliferative and pro-apoptotic effects of TGFβ on epithelial cell growth (Ellenrieder 2008). With respect to liver fibrosis, we previously reported that high-fat diet (HFD)-induced liver fibrosis was accompanied by increased KLF10 expression (Kim et al. 2014a). In the present study, we investigated whether KLF10 plays an important role in generation of liver fibrosis using *KLF10*-deleted transgenic mice and examined the impact of *KLF10* deletion in HCC development.

Materials and methods

Animal studies

KLF10 knockout (KO) mice were provided by Prof. Woon-Kyu Lee (Inha University College of Medicine, Incheon, Republic of Korea). The mice developed, grew, and reproduced normally, as previously described (Song et al. 2012; Subramaniam et al. 2005). *KLF10* KO mice were compared with wild-type (WT) C57BL/6 J mice. Each experimental group included ≥ 5 animals. Randomization was not used to allocate the animals to the control and treatment groups. All experimental animals that were properly sacrificed were included in the analysis. Investigators who performed the histologic analysis were blinded to the animals' group allocations.

The animal experimental procedures and protocols were approved by the Institutional Animal Care and Use Committee of Gangnam Severance Hospital, Yonsei University College of Medicine (permit nos.: 2013–0173 and 2015–0049). The study was performed in accordance with the guidelines of the Institutional Animal Care and Use Committee.

Liver fibrosis induction by HFD

Fatty liver-associated liver fibrosis was induced by feeding a diet high in saturated fats, cholesterol, and sucrose (i.e., HFD) as previously reported (JK Kim et al., 2014b). Male *KLF10* KO and WT mice were fed an HFD (#5053*; PicoLab, Bethlehem, PA, USA) consisting of 15% anhydrous milkfat, 1.0% cholesterol, and 50% sucrose. Either a standard diet (SD) or HFD was administered to 6-week-old mice for 24 weeks before sacrifice. All sacrificed animals were included in the analysis.

HCC induction

HCC was chemically induced using N-diethylnitrosamine (DEN). DEN produces reactive ethyl diazonium ions in the liver, altering the expression levels of tumor promoting and/or suppressing genes (Swenberg et al. 1991); this leads to HCC development without the onset of liver fibrosis (F Heindryckx et al., 2010; M Kushida et al. 2011). In DEN-induced mouse hepatocarcinogenesis, altered hepatocellular foci, such as glycogen-rich clear cells, have been used as markers of preneoplastic lesions (Kushida et al. 2011). In the present study, DEN was intraperitoneally administered once weekly to 2-week-old male *KLF10* KO and WT mice for 8 weeks. DEN was administered at a dose of 20 mg/kg bodyweight for 2 weeks, followed by 50 mg/kg bodyweight beginning at the age of 4 weeks; this treatment was continued for 6 weeks. Mice were sacrificed at the age of 24 weeks. Untreated age-matched WT mice were sacrificed and served as controls. All sacrificed animals were included in the analysis.

Histologic evaluation of animal liver samples

The liver samples from sacrificed animals were macroscopically evaluated before storage. HCC and non-HCC tissues were separately collected and snap-frozen in liquid nitrogen. Hematoxylin and eosin staining was

performed to evaluate morphological changes. Sirius red staining was used to evaluate fibrotic changes in the liver. Fibrosis was semi-quantitatively evaluated by expressing the fibrosis ratio using an image analysis system as described in a previous study with modification (O'Brien et al. 2000). The total area was the sum of the area of the microscopic fields, including the parenchyma and fibrosis. For each slide, the area of fibrosis was evaluated in 20 consecutive fields at a magnification of 40× and averaged.

Patients, tissues, immunohistochemistry

We retrospectively reviewed 277 patients with HCC who had undergone curative liver resection between January 2006 and December 2016 at Gangnam Severance Hospital, Yonsei University College of Medicine, Seoul, Korea. Paraffin-embedded HCC samples of 60 patients were subjected to histopathological analysis. This study protocol was approved by the Institutional Review Board of Gangnam Severance Hospital, Yonsei University College of Medicine (permit no.: 3-2015-0177). The need for informed consent was waived by the Institutional Review Board because the researchers only accessed the database for analysis purposes and all personal information was blinded by coding. Immunohistochemical staining was performed using mouse monoclonal antibody against KLF10 (sc-130408; Santa Cruz Biotechnology, Santa Cruz, CA, USA; 1:500 dilution) (Chang et al. 2012; Peng et al. 2019). Immunopositivity was assessed with respect to cellular localization, intensity, and distribution as previously described (Hsu et al. 2014; Pandya et al. 2004). KLF10 expression was quantified using a visual grading system based on the extent of staining (E) (percentage of tumor cells: 0, none; 1, 1–30%; 2, 31–60%; 3, > 60%) and intensity of staining (I) (0, none; 1, weak staining; 2, moderate staining; 3, strong staining). The E and I values were multiplied (E × I) to calculate the EI score (0–9). EI scores of < 3 and ≥ 3 indicated low and high expression levels, respectively.

Cell culture, transfection, and conditioned medium

The human HCC cell line Hep3B (KCLB #88064) (RRID: CVCL_0326) and human hepatic stellate cell line LX2 (cat #SCC064) (RRID: CVCL_5790) were purchased from Korean Cell Line Bank (Seoul, Republic of Korea). The human cell lines had been authenticated using short tandem repeat profiling within 3 years prior to this study. All experiments were performed using mycoplasma-free cells (EMD Millipore, Temecula, CA, USA), as previously described (Friedman et al. 1992; Hiron et al. 1992). Transient depletion assays were performed using DharmaFECT 1 (Dharmacon, Lafayette, CO, USA), in accordance with the manufacturer's recommendations. SmartPool siRNA against *KLF10* (L-006566-00) and control siRNA (D-001206-13) were purchased from Dharmacon. Briefly, 25 nM siRNA ON-TARGETplus SmartPool (L-006566-00) was transfected with a plating density of 3×10^5 cells per well in a six-well plate.

Transwell invasion assay and co-culture

The invasive abilities of Hep3B and LX2 cells were evaluated in vitro using a Transwell chamber system with 8.0-μm pore polycarbonate filter inserts (Corning Costar Corp., Cambridge, MA, USA), as previously described (Prenzel et al. 2011). The lower side of the filter was coated with 10 μL of gelatin (1 mg/mL), whereas the upper side was coated with 10 μL of Matrigel. The effect of KLF10 on cell invasion was investigated at 24 h after siRNA transfection by seeding 3×10^5 cells in the upper part of the filter. After 24 h of incubation at 37 °C with 5% CO_2, the upper surface of the membrane was scrubbed using a cotton swab; cells on the lower surface of the membrane were fixed with 4% paraformaldehyde, then stained with crystal violet. The numbers of cells that migrated through the Matrigel were counted in five random fields under a microscope at 200× magnification.

For co-culture of Hep3B and LX2 cells, cells were cultured using hanging cell culture inserts (pore size, 1 μm; Falcon) to separate the cell populations. Wells and inserts with media were stabilized for 24 h at 37 °C, in accordance with the manufacturer's recommendations. Hep3B cells were seeded in the insert (3×10^3 cells/cm^2) and incubated overnight in Dulbecco's modified Eagle medium with 10% fetal bovine serum. LX2 cells (3×10^5 cells/cm^2) were seeded on the upper part of the filter of the Transwell chamber system, then stabilized for 24 h. On the following day, LX2 cells were subjected to siRNA transfection (*KLF10* or control) using DharmaFECT 1 (Dharmacon), in accordance with the manufacturer's recommendations. The plate with LX2 cells was placed below the culture insert with Hep3B cells. The culture was continued for an additional 24 h, and the invasion assay was performed as previously described.

RNA isolation and real-time polymerase chain reaction (PCR)

Total RNA was extracted from frozen whole liver (in the HFD experiment), from the tumor sites of the liver (in the DEN experiment), or from isolated cells using TRIzol reagent (Invitrogen, Carlsbad, CA, USA) and Qiagen mini columns (Qiagen Inc., Valencia, CA, USA) in accordance with the manufacturer's recommendations. RNA samples were quantified via spectrophotometry. RNA integrity was assessed by agarose gel electrophoresis and ethidium bromide staining. The RNA samples were diluted in RNase-free water and stored at − 70 °C until use. In total, 5 μg of RNA were reverse-transcribed via

RNA PCR (version 1.2; TaKaRa Bio Inc., Tokyo, Japan) in accordance with the manufacturer's recommendations. Oligonucleotide primers and TaqMan probes for *TGFβ*, *SMAD2*, *SMAD3*, *SMAD7*, *collagen α1(I)* [*Col1α(I)*], *α smooth muscle actin (SMA)*, *lecithin retinol acyltransferase (Lrat)*, *E-cadherin*, *N-cadherin*, *SNAI2*, and *matrix metalloproteinases (MMPs) 2* and *9* were used; *18S* was used an internal control. Probes were obtained from Applied Biosystems (Perkin-Elmer/PE Applied Biosystems, Foster City, CA, USA) and prepared in ready-to-use format with Assays-on-Demand Gene Expression Products. TaqMan probes were labeled at the 5' end with the reporter dye FAM and at the 3' end with the minor groove binder nonfluorescent quencher. Quantitative PCR was performed in triplicate for each sample using the Step One Plus Real Time System (Applied Biosystems). Each 20-μL reaction was performed using 10 μL of TaqMan Fast Universal Master Mix (Applied Biosystems, Darmstadt, Germany), 1 μL of Gene Expression Mix, and 2 μL of cDNA diluted in 7 μL of RNase-free water. The thermocycler protocol was 20 s at 95 °C, followed by 40 cycles of 5 s at 95 °C and 20 s at 60 °C. The fold-change in mRNA expression levels of target genes relative to the endogenous 18S control was calculated as previously described (KJ Livak and TD Schmittgen, 2001).

Statistical analysis

All results are presented as means ± standard errors of the mean. Data were analyzed using nonparametric tests (Kruskal–Wallis or Mann–Whitney) or one-way analysis of variance with Tukey's post hoc test. For patients, overall survival was analyzed according to KLF10 expression using the Kaplan–Meier method. Differences in survival rate were compared using the log-rank test. *P*-values < 0.05 were considered statistically significant. Statistical analysis was performed using SPSS software (version 23; IBM Corp., Armonk, NY, USA).

Results

Effect of *KLF10* deletion on TGFβ signaling in the untreated liver

KLF10 is a critical effector of the TGFβ/SMAD signaling pathway (Johnsen et al. 2002b). Male WT mice (n = 5) and *KLF10* KO mice (n = 5) fed an SD were sacrificed at the age of 8 weeks to evaluate the effect of *KLF10* deletion on gene expression. In *KLF10* KO mice, the liver exhibited increased expression levels of *TGFβ*, *SMAD2*, and the inhibitory factor *SMAD7*, although the expression of *SMAD3* was unaffected (Fig. 1A). αSMA is upregulated in activated hematopoietic stem cells (HSCs) and is closely associated with liver fibrosis (N Roehlen et al., 2020). In untreated *KLF10*-deleted mice, the liver exhibited significantly upregulated expression of *αSMA*; the expression of *Lrat*, which is expressed in quiescent HSCs, was unaffected (Fig. 1B).

KLF10 deletion did not alter HFD-induced liver fibrosis

Liver fibrosis and cirrhosis are strong predisposing factors for HCC (EAS Liver 2018; Marrero et al. 2018). Additionally, TGFβ facilitates liver fibrosis. Studies have shown that TGFβ is important for the activation and proliferation of HSCs, which are the main cellular components of liver fibrosis (Greuter and Shah 2016). Additionally, we have shown that HFD-induced liver fibrosis is accompanied by increased KLF10 expression (JK Kim et al., 2014a). Therefore, we investigated how *KLF10* deletion affected TGFβ signaling and liver fibrosis in mice with HFD-induced chronic liver inflammation. Male *KLF10* WT (n = 6) and KO (n = 5) mice were fed an HFD, high in saturated fats, cholesterol, and sucrose,

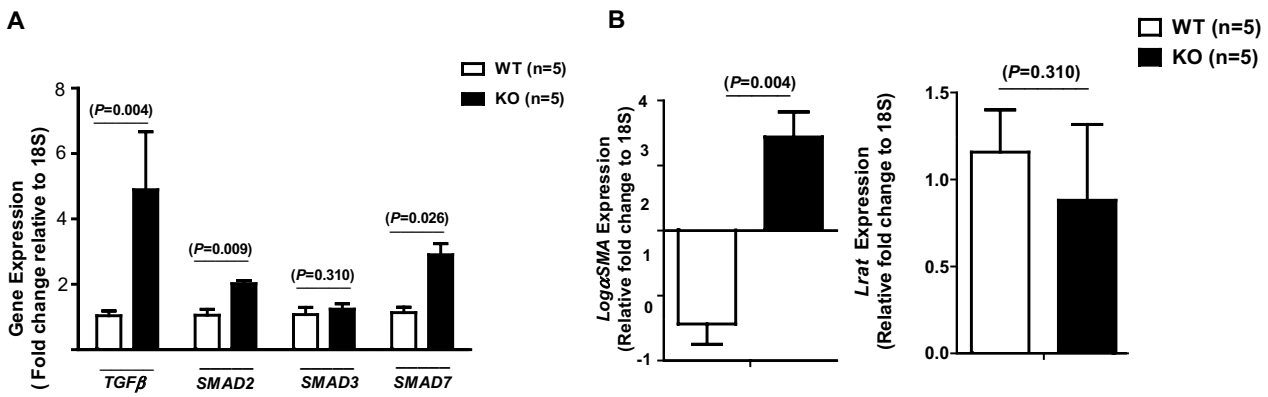

Fig. 1 Gene expression in the untreated liver of *KLF10* wild-type (WT) and knockout (KO) mice. **A** The expression of TGFβ-related signaling genes was evaluated by real-time polymerase chain reaction in WT (n = 5) and *KLF10* KO (n = 5) mice liver with no treatment. **B** The expression of hepatic stellate cell activation-related genes was compared between WT (n = 5) and *KLF10* KO (n = 5) mice liver with no treatment

for 24 weeks; male WT mice (n = 6) and KO (n = 5) were fed an SD for 24 weeks and served as controls. The HFD increased liver fibrosis, as evaluated by Sirius red staining (Fig. 2A), as well as the mRNA expression level of *Col1α* in the livers of *KLF10* WT and KO mice, without significant differences between groups (Fig. 2B). In both WT and KO mice, the provision of an HFD induced increases in the expression levels of *TGFβ* and downstream signals *SMAD3* compared with the SD-fed controls (Fig. 2C). Although the HFD-fed WT mice showed increased *SMAD2* and *SMAD7* expression, the HFD-fed KO mice did not show significant increases compared with the SD-fed KO controls. *TGFβ*, *SMAD2*, and *SMAD7* expression levels were significantly higher in *KLF10* KO control mice than in WT mice, whereas *SMAD3* expression levels showed no significant differences. *TGFβ* and *SMAD2* expression were significantly higher in HFD-fed *KLF10* KO than in HFD-fed WT mice. Overexpression of *αSMA* was observed in the livers of HFD-treated WT and *KLF10* KO mice, without significant differences between the groups (Fig. 2D).

KLF10 deletion increased the liver cancer burden in DEN-treated mice

In the present study, 2-week-old male *KLF10* KO (n = 9) and WT (n = 8) mice received weekly intraperitoneal injections of DEN for 6 weeks. DEN-injected mice were sacrificed at the age of 24 weeks. Age-matched male WT mice without any treatment (n = 8) served as controls. Liver specimens were stained with hematoxylin and eosin, then evaluated for HCC development (Fig. 3A). HCC nodules were counted and measured via microscopy at a low magnification. The HCC burden was defined as the longest diameter of the tumor (mm) × tumor number for each liver specimen. When HCC was induced by DEN treatment, *KLF10* deletion resulted in a significantly greater tumor burden compared with the burden in DEN-treated WT mice (Fig. 3B). The extent of liver fibrosis did not significantly differ between groups (Fig. 3C). DEN treatment was associated with increased *TGFβ*, *SMAD3*, and *SMAD7* expression in both DEN-treated WT and KO mice compared with their untreated counter parts (Fig. 4A). However, there were no significant differences in the extent of the increment between DEN-treated WT and KO mice. *SMAD2* expression was significantly upregulated by *KLF10* deletion, and treatment

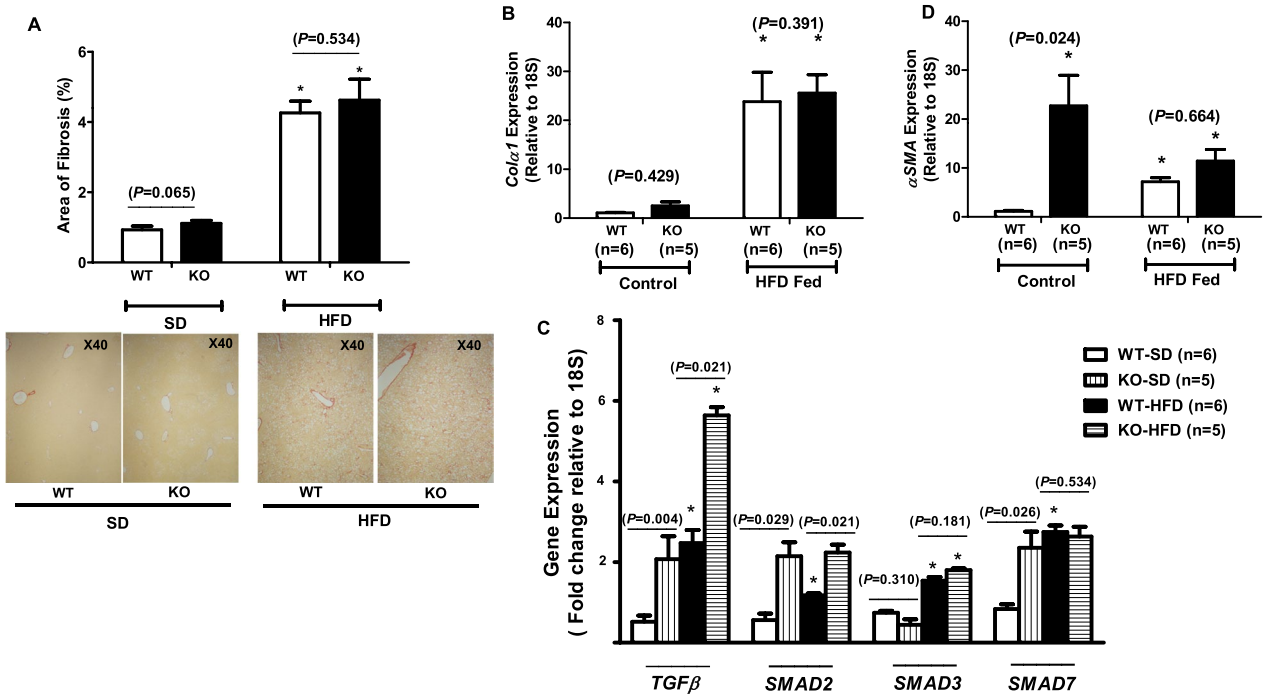

Fig. 2 Liver fibrosis induction and gene expression in high-fat diet (HFD)-treated liver of *KLF10* wild-type (WT) and knockout (KO) mice. **A** Liver tissue was stained for collagen deposition using Sirius red staining, and a morphometric analysis was performed. **B** The expression of *Cola1* was evaluated by real-time polymerase chain reaction in WT mice fed a standard diet (SD) (n = 6), *KLF10* KO mice fed an SD (n = 5), WT mice fed an HFD (n = 6), and *KLF10* KO mice fed an HFD (n = 5). **C** Expression of TGFβ-related signaling genes. **D** Expression of *αSMA*. *$P < 0.005$ compared with SD-fed WT or KO mice

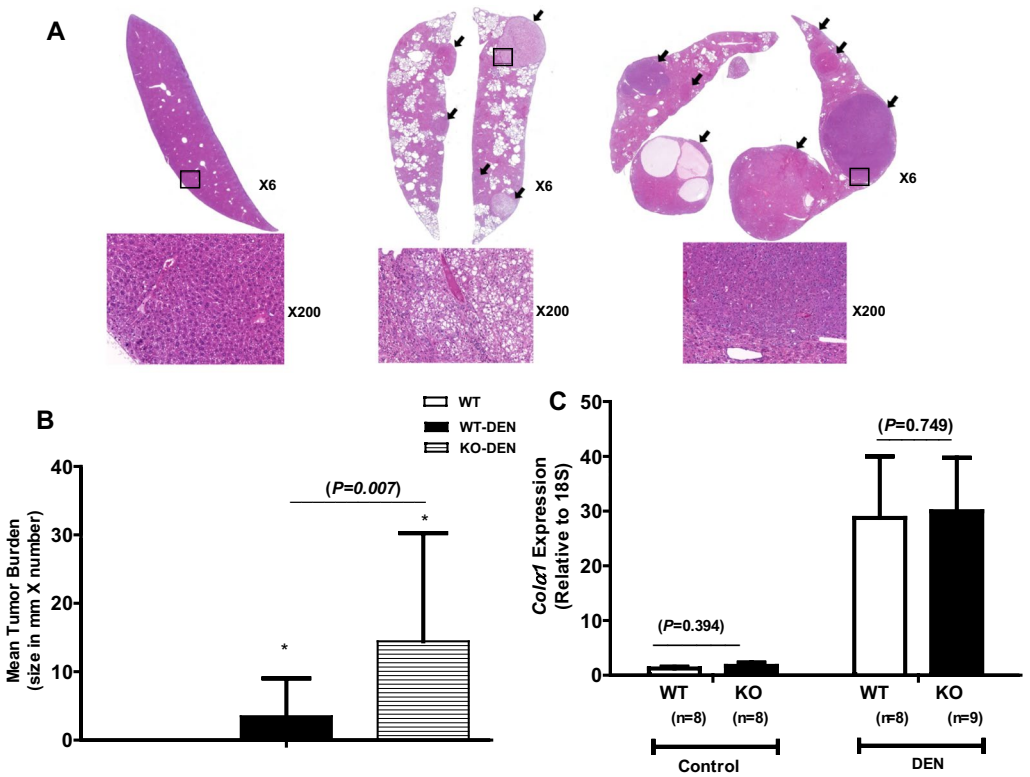

Fig. 3 Induction of hepatocellular carcinoma (HCC) by diethylnitrosamine (DEN) treatment in *KLF10* wild-type (WT) and knockout (KO) mice. **A** Two-week-old *KLF10* KO (n = 9) and WT (n = 8) mice received intraperitoneal DEN injections weekly for 8 weeks. DEN-injected mice were sacrificed at the age of 24 weeks. Liver specimens were stained with hematoxylin and eosin (H&E) and evaluated for HCC development. Representative images of HCC (arrow) are shown. The boxed part of HCC in the low-magnification image (6×) is magnified (200×) and presented. **B** The HCC burden (size in mm × tumor number) was evaluated under microscopy after H&E staining in *KLF10* WT (n = 8) and KO (n = 9) mice. (**C** Assessment of liver fibrosis by *Cola1* mRNA expression after DEN treatment in *KLF10* WT (n = 8) and KO (n = 9) mice within liver tumor sites. Age-matched WT (n = 8) or KO (n = 8) mice with no treatment served as the controls. **P* < 0.005 compared with SD-fed WT or KO mice

with DEN induced a further increase in *SMAD2* expression (Fig. 4A).

KLF10 deletion upregulated markers of mesenchymal cells in the liver

To explore how *KLF10* deletion promotes HCC development in DEN-treated mice, we evaluated the expression levels of *αSMA, E-cadherin, N-cadherin,* and *SNAI2* (i.e., markers of epithelial-to-mesenchymal transition [EMT]). DEN-treated WT mice exhibited increased expression levels of *αSMA*, *E-cadherin,* and *SNAI2* (Fig. 4B). *KLF10* deletion resulted in increased *αSMA*, *E-cadherin, N-cadherin,* and *SNAI2*. Although DEN treatment in *KLF10* KO mice further increased *αSMA*, *N-cadherin,* and *SNAI2* expression, the level of *E-cadherin* did not show significant alteration after DEN treatment (Fig. 4B).

KLF10 deletion enhanced HCC invasiveness genes

MMPs facilitate EMT by increasing invasion and metastasis (BN Smith and NA Bhowmick, 2016). Although not typically present in liver cells, MMP2 is expressed in HCC; in this context, it enhances tumor invasion and metastasis (Chen et al. 2017; Chen et al. 2012). MMP9 and MMP2 are poor prognostic factors in HCC. *KLF10* deletion resulted in enhanced *MMP2* and *MMP9* gene expression in untreated KO mice, and DEN treatment further increased *MMP9* expression in *KLF10* KO mice (Fig. 4C). In *KLF10* WT mice, DEN treatment was associated with increased *MMP2* and *MMP9* expression (Fig. 4C). However, because untreated *KLF10* KO mice already had increased *MMP2* and *MMP9* levels, the levels of both *MMP2* and *MMP9* in DEN-treated WT mice remained lower than those in DEN-treated KO mice.

KLF10-depleted LX2 cells promote invasiveness in Hep3B cells

The effect of *KLF10* depletion on the invasiveness of Hep3B and LX2 cells was evaluated using siRNA. *KLF10* depletion promoted invasion in Hep3B and LX2 cells (Fig. 5A). Activated HSCs are important cellular components in the tumor microenvironment (Coulouarn and Clement 2014; Friedman 2008). A previous study

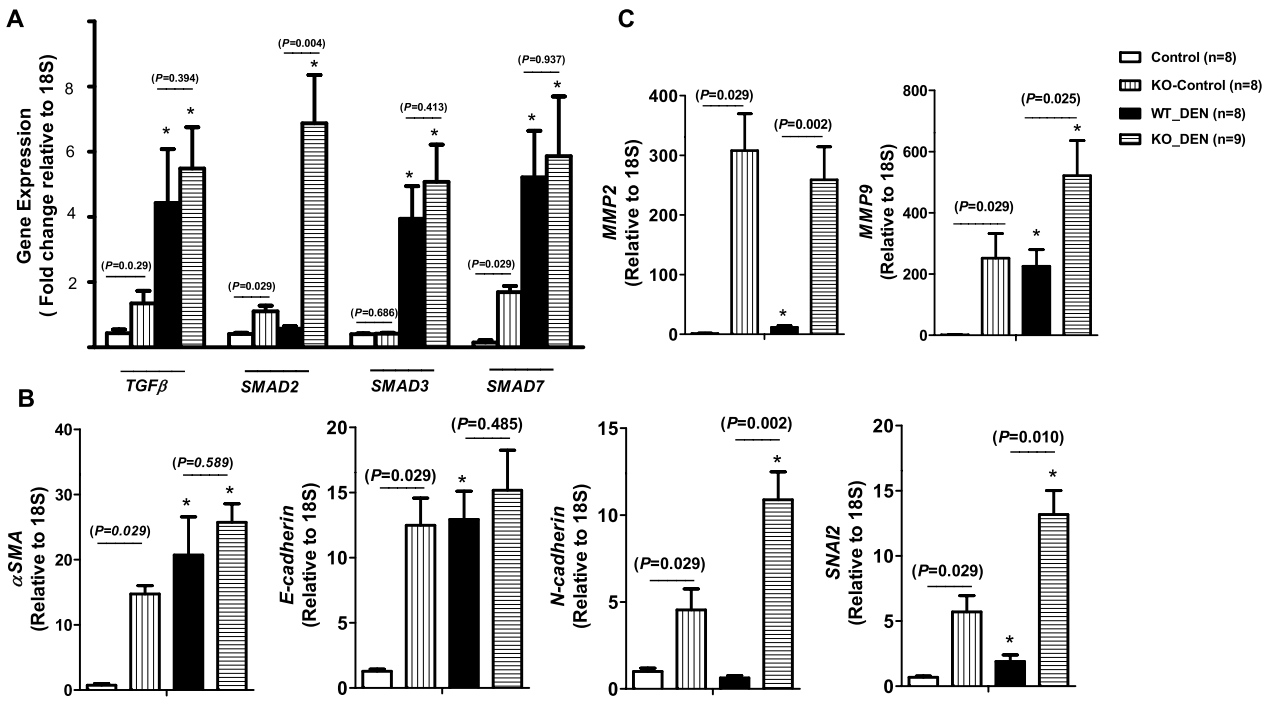

Fig. 4 Gene expression in tumor sites of diethylnitrosamine (DEN)-treated liver of *KLF10* wild-type (WT) and knockout (KO) liver. **A** The expression of TGFβ-related signaling genes was measured in WT mice without treatment (n = 8), KO mice without treatment (n = 8), WT mice with DEN treatment (n = 8), and KO mice with DEN treatment (n = 9). **B** The expression of epithelial-to-mesenchymal transition–related markers was evaluated. **C** The expression of genes related to tumor invasiveness was assessed. *$P < 0.005$ compared with SD-fed WT or KO mice

revealed that when co-cultured with HSCs, HCC cells exhibited significant increases in proliferation and migration (Amann et al. 2009). To determine whether *KLF10* depletion alters the effects of HSCs on Hep3B, Hep3B cells were co-cultured with *KLF10*-preserved or *KLF10*-depleted HSCs. The invasiveness of Hep3B cells was significantly enhanced during co-culture with *KLF10*-depleted LX2 cells (Fig. 5B).

Low KLF10 expression in human HCC is associated with poor survival

Patients who underwent liver resection for treatment of HCC from January 2006 to December 2016 were retrospectively evaluated. Of 277 patients, 60 patients with HCC who underwent curative liver resection with a follow-up period of > 12 months were selected, and HCC samples were subjected to histopathological analysis. These 60 patients' demographic findings are presented in Table 1. The EI score ranged from 0 to 9, with EI scores of < 3 and ≥ 3 indicating low and high expression levels, respectively. Compared with a high EI score, a low EI score was associated with a significantly lower survival rate (Fig. 6A). While immunohistochemistry revealed strong KLF10 expression in the non-tumor hepatocytes, the tumor site showed various intensities and extents of KLF10 staining. Representative images of KLF10-positive tumor cells are shown in Fig. 6B.

Discussion

This study showed that *KLF10* deletion resulted in an increased incidence of DEN-induced HCC in mice, without the onset of liver fibrosis. Loss of KLF10 led to enhanced migration of malignant hepatocytes and hepatic stellate cells.

KLF10, a TGFβ early responsive gene, is involved in a positive feedback loop with respect to TGFβ signaling. Therefore, we hypothesized that modulation of *KLF10* expression would alter the extent of liver fibrosis in a HFD-induced fatty liver mice model. Unexpectedly, HFD challenge did not lead to worsening of liver fibrosis in *KLF10* KO mice compared with WT mice. Although the livers from both HFD-treated WT and *KLF10* KO mice showed increased expression of *TGFβ* and *SMAD3* compared with those of the respective controls, *TGFβ* of HFD-treated *KLF10* KO mice was further increased compared with that of HFD-treated WT mice. The increase in *SMAD3* in WT and KO mice after DEN treatment showed no significant differences between the two groups. *SMAD2* and *SMAD3* have both overlapping and distinct roles in the TGFβ signaling pathway; a previous study showed that *SMAD3* is important for collagen

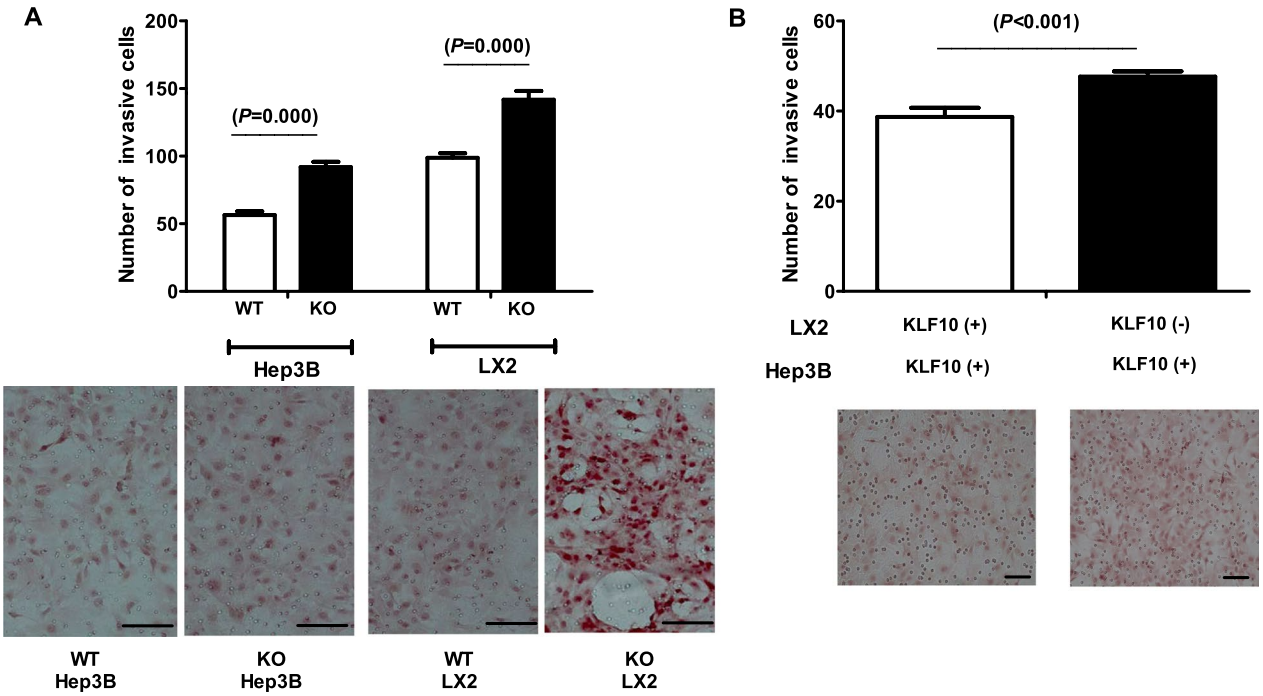

Fig. 5 Invasion of Hep3B and LX2 cells. **A** Invasion of Hep3B and LX2 cells was determined using the Transwell assay. Transient *KLF10* deletion was induced using siRNA. The number of invasive cells was counted in five random fields under a microscope at 200× magnification and is shown as the mean ± standard deviation. Representative images from the experiment are shown. **B** Invasion of Hep3B cells was assessed after co-culture with LX2 cells with *KLF10* either deleted or preserved. Hep3B and LX2 cells were cultured using hanging cell culture inserts (1-μm pore size, Falcon) to separate cell populations. Hep3B cells were seeded in the insert (3×10^3 cells/cm^2) and allowed to attach overnight in Dulbecco's modified Eagle medium with 10% fetal bovine serum. LX2 cells (3×10^5 cells/cm^2) were seeded on the upper part of the filter of the Transwell chamber system, and siRNA transfection (*KLF10* or control) was performed. The plate with LX2 cells was placed below the culture insert with Hep3B cells. The number of invasive cells was counted in five fields under a microscope at 200× magnification and is shown as the mean ± standard deviation. Representative images from the experiment are shown. Scale bar = 50 μm

production by HSCs (Zhang et al. 2015). The lack of a significant difference in *SMAD3* expression after DEN treatment in WT and KO mice may partially explain the absence of changes in liver fibrosis after *KLF10* deletion. Because KLF10 is reportedly involved in a positive feedback loop of TGFβ signaling, increased TGFβ expression in the liver of *KLF10* KO mice was not expected. However, cellular responses involving both TGFβ and KLF10 are dependent on the cell type (Itoh and ten Dijke 2007), and TGFβ expression was significantly increased after hepatectomy in *KLF10* KO mice (Heo et al. 2017). Thus, a further study with a different fibrosis model is necessary.

Although our results did not reveal a significant effect of *KLF10* deletion on liver fibrogenesis, the loss of KLF10 led to increased incidence of DEN-induced HCC in mouse liver, suggesting that KLF10 has a tumor suppressor role. Our animal experimental results are in accordance with the result of KLF10 expression in the human HCC specimens, showing decreased survival with decreased KLF10 expression after HCC resection. Additionally, our study provides evidence that KLF10 has a suppressive role during HCC development and progression. The loss of KLF10 led to the upregulation of genes associated with EMT and tumor metastasis. EMT is a transdifferentiation process with a central roles in cancer metastasis and the development of stem cell-like features (Valastyan and Weinberg 2011). TGFβ is among the most potent inducers of EMT; in vitro analyses have shown that stimulation of primary hepatocytes with TGFβ can induce EMT (Caja et al. 2011; Dooley et al. 2008). The loss of KLF10 led to significant upregulation of *TGFβ* and other mesenchymal markers, such as *SNAI2* and *N-cadherin,* in mouse liver after DEN treatment. MMPs have key roles in promoting the invasive and metastatic abilities of malignant tumor cells. MMP2 is not typically present in liver cells but is expressed in HCC cells (Wang et al. 2014). Similar to MMP2, MMP9 plays a major role in tumor angiogenesis. MMP9 overexpression in HCC leads to a higher TNM stage and a poor prognosis (Chen et al. 2012). The present study revealed significantly higher expression levels of *MMP2* and *MMP9* after *KLF10* deletion in the liver of DEN-treated mice, compared with the liver of *KLF10*-preserved WT mice. In addition to the in vivo findings, our in vitro

Table 1 Baseline characteristics of patients that underwent liver resection due to HCC

Variables	n = 60
Age, years, median (range)	51 (30–81)
Gender (M:F)	49:11
Etiology of liver disease	
HBV	43 (71.7)
HCV	4 (6.7)
Others	13 (21.7)
Serum AFP, ng/mL (%)	
< 200	53 (88.3)
≥ 200	7 (11.7)
Tumor number (%)	
Single	52 (86.7)
Multiple	8 (13.3)
Tumor size	
≤ 5 cm	52 (86.7)
> 5 cm	8 (13.3)
Existence of microvascular invasion (%)	16 (26.7)
Edmonson grade (%)	
Grade 1, 2	25 (41.7)
Grade 3, 4	35 (58.3)
Existence of Pathologic Cirrhosis (%)	48 (80.0)
KLF10 Expression	
High	54 (90.0)
Low	6 (10.0)

AFP alpha-fetoprotein; *KLF10* Kruppel-like factor 10

experiment revealed increased migration of Hep3B cells after siRNA-mediated depletion of *KLF10*.

Activated HSCs promote the proliferation and migration of liver cancer cells, both in vivo and in vitro (Amann et al. 2009). Our study revealed increased migration of Hep3B cells co-cultured with *KLF10*-depleted LX2 cells compared with the migration of Hep3B cells co-cultured with *KLF10*-intact LX2 cells. These findings suggest that *KLF10* deletion facilitates the migration of liver cancer cells and enhances the tumorigenic effect of the cancer microenvironment. However, the results of our study regarding the effect of KLF10 loss on liver fibrosis and HCC development should be validated by different fibrosis and HCC models because some etiologies of chronic liver disease are more likely to induce liver fibrosis and HCC in clinical settings (Giannelli et al. 2014).

Conclusion

The results of this study suggest that loss of KLF10 facilitates liver cancer development with alteration in TGFβ signaling. Loss of KLF10 led to the upregulation of the mesenchymal cell markers *N-cadherin* and *SNAI2* and the invasiveness markers *MMP2* and *MMP9*. *KLF10* inhibition enhanced the metastatic function of liver cancer cells and the tumor-enabling function of HSCs. In addition, *KLF10*-depleted liver cancer cells and HSCs demonstrated increased invasiveness. These results support the idea that KLF10 is involved in the tumor-suppressing role of TGFβ and

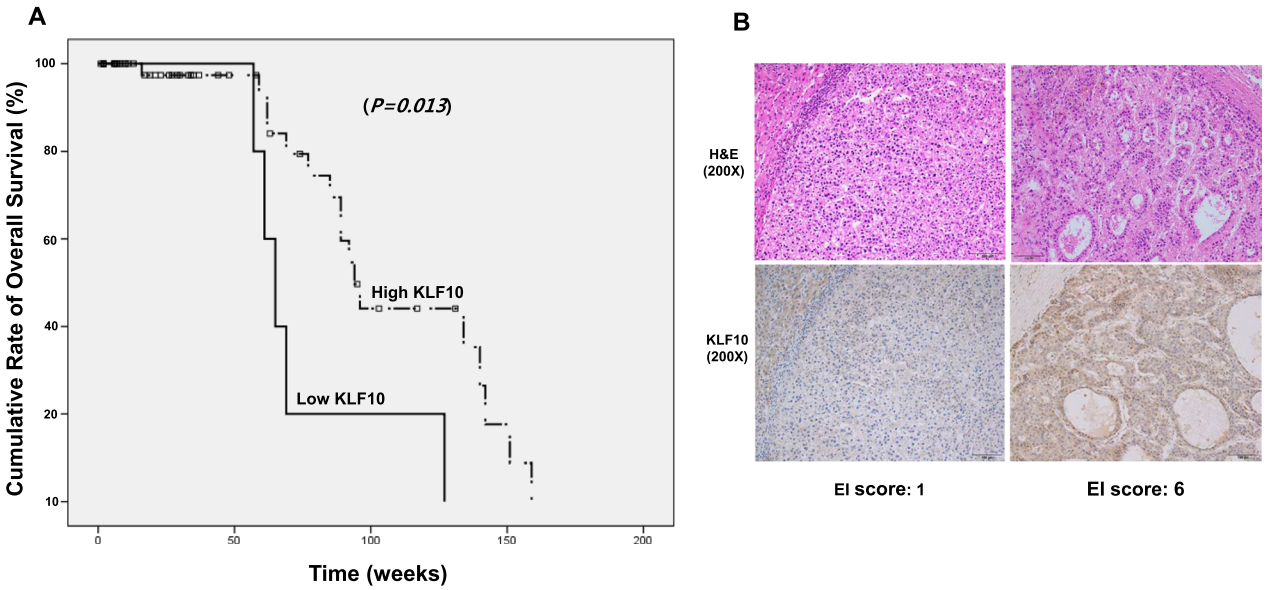

Fig. 6 Survival of patients after curative HCC resection according to KLF10 expression in the resected tumor after immunohistochemical staining. **A** The combination of the extent (E) and intensity (I) of staining was obtained by calculating E × I to give the EI score, which ranged from 0 to 9. EI scores < 3 indicated low expression, and EI scores ≥ 3 indicated high expression. **B** Representative immunohistochemistry of KLF10 in human HCC tissue of high and low EI score immunostaining are shown

that loss of KLF10 promotes cancer development and progression. However, this study involved only a single HCC animal model, and a relatively small number of human samples with a limited follow-up period. Further studies using different HCC models and other cohorts of patients with HCC are necessary to validate our results and investigate the role of KLF10 in HCC.

Abbreviations

αSMA	Alpha smooth muscle actin
DEN	Diethylnitrosamine
EMT	Epithelial-to-mesenchymal transition
HCC	Hepatocellular carcinoma
HFD	High-fat diet
KO	Knockout
Lrat	Lecithin retinol acyltransferase
MMP	Matrix metalloproteinase
SD	Standard diet
TGF	Transforming growth factor
TIEG	Transforming growth factor β inducible early gene
WT	Wild type

Acknowledgements
Not applicable.

Author contributions
JIL and WKL conceived and designed the study; SHY, HYC, and HWL performed the experiments and acquired the data; JIL analyzed and interpreted the data; KWL critically reviewed the study; and SHW and JIH drafted the manuscript.

Funding
This study was supported by the Basic Science Research Program through the National Research Foundation of Korea (NRF) funded by the Ministry of Science, ICT & Future Planning (NRF-2016R1A2B4015192) and the Faculty Research Grant of Yonsei University College of Medicine (62015-0034).

Availability of data and materials
The data that support the findings of this study are available from the corresponding author upon reasonable request.

Declarations

Ethics approval and consent to participate
The animal experimental procedures and protocols were approved by the Institutional Animal Care and Use Committee of Gangnam Severance Hospital, Yonsei University College of Medicine (permit nos.: 2013-0173 and 2015-0049). The study was performed in accordance with the guidelines of the Institutional Animal Care and Use Committee. The protocol of the study using human HCC specimens was approved by the Institutional Review Board of Gangnam Severance Hospital, Yonsei University College of Medicine (permit no.: 3-2015-0177). The need for informed consent was waived by the Institutional Review Board because the researchers only accessed the database for analysis purposes and all personal information was blinded by coding.

Consent for publication
All authors agree to publish these data.

Competing interests
The authors declare no competing interests.

Received: 10 May 2023 Accepted: 30 October 2023
Published online: 09 November 2023

References

Alter HJ, Seeff LB. Recovery, persistence, and sequelae in hepatitis C virus infection: a perspective on long-term outcome. Semin Liver Dis. 2000;20(1):17–35.
Amann T, Bataille F, Spruss T, Muhlbauer M, Gabele E, Scholmerich J, et al. Activated hepatic stellate cells promote tumorigenicity of hepatocellular carcinoma. Cancer Sci. 2009;100(4):646–53.
Caja L, Conrad O, Esther B, Murillo MM, Miro-Obradors MJ, Palacios E, et al. Differential intracellular signalling induced by TGF-beta in rat adult hepatocytes and hepatoma cells: Implications in liver carcinogenesis. Cell Signal. 2007;19(4):683–94.
Caja L, Bertran E, Campbell J, Fausto N, Fabregat I. The transforming growth factor-beta (TGF-beta) mediates acquisition of a mesenchymal stem cell-like phenotype in human liver cells. J Cell Physiol. 2011;226(5):1214–23.
Caldwell SH, Crespo DM, Kang HS, Al-Osaimi AM. Obesity and hepatocellular carcinoma. Gastroenterology. 2004;127(5 Suppl 1):S97-103.
Chang VHS, Chu PY, Peng SL, Mao TL, Shan YS, Hsu CF, et al. Kruppel-like factor 10 expression as a prognostic indicator for pancreatic adenocarcinoma. Am J Pathol. 2012;181(2):423–30.
Chen R, Cui J, Xu C, Xue T, Guo K, Gao D, et al. The significance of MMP-9 over MMP-2 in HCC invasiveness and recurrence of hepatocellular carcinoma after curative resection. Ann Surg Oncol. 2012;19(Suppl 3):S375–84.
Chen G, Qin GH, Dang YW, Yang J. The prospective role of matrix metalloproteinase-2/9 and transforming growth factor beta 1 in accelerating the progression of hepatocellular carcinoma. Transl Cancer Res. 2017;6:S229–31.
Coulouarn C, Clement B. Stellate cells and the development of liver cancer: therapeutic potential of targeting the stroma. J Hepatol. 2014;60(6):1306–9.
Dewidar B, Meyer C, Dooley S, Meindl-Beinker AN. TGF-beta in hepatic stellate cell activation and liver fibrogenesis-updated 2019. Cells. 2019;8(11):1419.
Dooley S, Hamzavi J, Ciuclan L, Godoy P, Ilkavets I, Ehnert S, et al. Hepatocyte-specific Smad7 expression attenuates TGF-beta-mediated fibrogenesis and protects against liver damage. Gastroenterology. 2008;135(2):642–59.
Ellenrieder V. TGFbeta regulated gene expression by Smads and Sp1/KLF-like transcription factors in cancer. Anticancer Res. 2008;28(3A):1531–9.
Fabregat I, Moreno-Caceres J, Sanchez A, Dooley S, Dewidar B, Giannelli G, et al. TGF-beta signalling and liver disease. FEBS J. 2016;283(12):2219–32.
Friedman SL. Hepatic stellate cells: protean, multifunctional, and enigmatic cells of the liver. Physiol Rev. 2008;88(1):125–72.
Friedman SL, Rockey DC, McGuire RF, Maher JJ, Boyles JK, Yamasaki G. Isolated hepatic lipocytes and Kupffer cells from normal human liver: morphological and functional characteristics in primary culture. Hepatology. 1992;15(2):234–43.
Giannelli G, Rani B, Dituri F, Cao Y, Palasciano G. Moving towards personalised therapy in patients with hepatocellular carcinoma: the role of the microenvironment. Gut. 2014;63(10):1668–76.
Greuter T, Shah VH. Hepatic sinusoids in liver injury, inflammation, and fibrosis: new pathophysiological insights. J Gastroenterol. 2016;51(6):511–9.
Heindryckx F, Mertens K, Charette N, Vandeghinste B, Casteleyn C, Van Steenkiste C, et al. Kinetics of angiogenic changes in a new mouse model for hepatocellular carcinoma. Mol Cancer. 2010. https://doi.org/10.1186/1476-4598-9-219.
Heo SH, Jeong ES, Lee KS, Seo JH, Lee WK, Choi YK. Knockout of kruppel-like factor 10 suppresses hepatic cell proliferation in a partially hepatectomized mouse model. Oncol Lett. 2017;13(6):4843–8.
Hiron M, Daveau M, Arnaud P, Bauer J, Lebreton JP. The human hepatoma Hep3B cell line as an experimental model in the study of the long-term regulation of acute-phase proteins by cytokines. Biochem J. 1992;287(Pt 1):255–9.
Hsu HT, Wu PR, Chen CJ, Hsu LS, Yeh CM, Hsing MT, et al. High cytoplasmic expression of kruppel-like factor 4 is an independent prognostic factor of better survival in hepatocellular carcinoma. Int J Mol Sci. 2014;15(6):9894–906.
Itoh S, ten Dijke P. Negative regulation of TGF-beta receptor/Smad signal transduction. Curr Opin Cell Biol. 2007;19(2):176–84.
Johnsen SA, Subramaniam M, Janknecht R, Spelsberg TC. TGFbeta inducible early gene enhances TGFbeta/Smad-dependent transcriptional responses. Oncogene. 2002a;21(37):5783–90.
Johnsen SA, Subramaniam M, Katagiri T, Janknecht R, Spelsberg TC. Transcriptional regulation of Smad2 is required for enhancement of TGFbeta/

Smad signaling by TGFbeta inducible early gene. J Cell Biochem. 2002b;87(2):233–41.
Kim JK, Lee KS, Chang HY, Lee WK, Lee JI. Progression of diet induced nonalcoholic steatohepatitis is accompanied by increased expression of kruppel-like-factor 10 in mice. J Transl Med. 2014. https://doi.org/10.1186/1479-5876-12-186.
Kim JK, Lee KS, Lee DK, Lee SY, Chang HY, Choi J, et al. Omega-3 polyunsaturated fatty acid and ursodeoxycholic acid have an additive effect in attenuating diet-induced nonalcoholic steatohepatitis in mice. Exp Mol Med. 2014;46:e127.
Kushida M, Kamendulis LM, Peat TJ, Klaunig JE. Dose-related induction of hepatic preneoplastic lesions by diethylnitrosamine in C57BL/6 mice. Toxicol Pathol. 2011;39(5):776–86.
Lee JI, Wright JH, Johnson MM, Bauer RL, Sorg K, Yuen S, et al. Role of Smad3 in platelet-derived growth factor-C-induced liver fibrosis. Am J Physiol Cell Physiol. 2016;310(6):C436–45.
Livak KJ, Schmittgen TD. Analysis of relative gene expression data using real-time quantitative PCR and the 2(T)(-Delta Delta C) method. Methods. 2001;25(4):402–8.
Liver EAS. EASL clinical practice guidelines: management of hepatocellular carcinoma. J Hepatol. 2018;69(1):182–236.
Llovet JM, Kelley RK, Villanueva A, Singal AG, Pikarsky E, Roayaie S, et al. Hepatocellular carcinoma. Nat Rev Dis Primers. 2021. https://doi.org/10.1038/s41572-020-00240-3.
Marrero JA, Kulik LM, Sirlin CB, Zhu AX, Finn RS, Abecassis MM, et al. Diagnosis, staging, and management of hepatocellular carcinoma: 2018 practice guidance by the american association for the study of liver diseases. Hepatology. 2018;68(2):723–50.
O'Brien MJ, Keating NM, Elderiny S, Cerda S, Keaveny AP, Afdhal NH, et al. An assessment of digital image analysis to measure fibrosis in liver biopsy specimens of patients with chronic hepatitis C. Am J Clin Pathol. 2000;114(5):712–8.
Pandya AY, Talley LI, Frost AR, Fitzgerald TJ, Trivedi V, Chakravarthy M, et al. Nuclear localization of KLF4 is associated with an aggressive phenotype in early-stage breast cancer. Clin Cancer Res. 2004;10(8):2709–19.
Peng T, Deng X, Tian F, Li ZH, Jiang P, Zhao X, et al. The interaction of LOXL2 with GATA6 induces VEGFA expression and angiogenesis in cholangiocarcinoma. Int J Oncol. 2019;55(3):657–70.
Prenzel T, Begus-Nahrmann Y, Kramer F, Hennion M, Hsu C, Gorsler T, et al. Estrogen-dependent gene transcription in human breast cancer cells relies upon proteasome-dependent monoubiquitination of histone H2B. Can Res. 2011;71(17):5739–53.
Roehlen N, Crouchet E, Baumert TF. Liver fibrosis: mechanistic concepts and therapeutic perspectives. Cells. 2020;9(4):875.
Russell WE, Coffey RJ Jr, Ouellette AJ, Moses HL. Type beta transforming growth factor reversibly inhibits the early proliferative response to partial hepatectomy in the rat. Proc Natl Acad Sci U S A. 1988;85(14):5126–30.
Smith BN, Bhowmick NA. Role of EMT in metastasis and therapy resistance. J Clin Med. 2016;5(2):17.
Song KD, Kim DJ, Lee JE, Yun CH, Lee WK. KLF10, transforming growth factor-beta-inducible early gene 1, acts as a tumor suppressor. Biochem Biophys Res Commun. 2012;419(2):388–94.
Subramaniam M, Harris SA, Oursler MJ, Rasmussen K, Riggs BL, Spelsberg TC. Identification of a novel TGF-beta-regulated gene encoding a putative zinc finger protein in human osteoblasts. Nucleic Acids Res. 1995;23(23):4907–12.
Subramaniam M, Gorny G, Johnsen SA, Monroe DG, Evans GL, Fraser DG, et al. TIEG1 null mouse-derived osteoblasts are defective in mineralization and in support of osteoclast differentiation in vitro. Mol Cell Biol. 2005;25(3):1191–9.
Swenberg JA, Hoel DG, Magee PN. Mechanistic and statistical insight into the large carcinogenesis bioassays on N-nitrosodiethylamine and N-nitrosodimethylamine. Can Res. 1991;51(23):6409–14.
Valastyan S, Weinberg RA. Tumor metastasis: molecular insights and evolving paradigms. Cell. 2011;147(2):275–92.
Valdes F, Murillo MM, Valverde AM, Herrera B, Sanchez A, Benito M, et al. Transforming growth factor-beta activates both pro-apoptotic and survival signals in fetal rat hepatocytes. Exp Cell Res. 2004;292(1):209–18.
Wang B, Ding YM, Fan P, Wang B, Xu JH, Wang WX. Expression and significance of MMP2 and HIF-1alpha in hepatocellular carcinoma. Oncol Lett. 2014;8(2):539–46.
West J, Card TR, Aithal GP, Fleming KM. Risk of hepatocellular carcinoma among individuals with different aetiologies of cirrhosis: a population-based cohort study. Aliment Pharmacol Ther. 2017;45(7):983–90.
Wilkes MC, Mitchell H, Penheiter SG, Dore JJ, Suzuki K, Edens M, et al. Transforming growth factor-beta activation of phosphatidylinositol 3-kinase is independent of Smad2 and Smad3 and regulates fibroblast responses via p21-activated kinase-2. Can Res. 2005;65(22):10431–40.
Zhang L, Liu CW, Meng XM, Huang C, Xu FY, Li J. Smad2 protects against TGF-beta 1/Smad3-mediated collagen synthesis in human hepatic stellate cells during hepatic fibrosis. Mol Cell Biochem. 2015;400(1–2):17–28.

Publisher's Note